

## Anelastic relaxation due to single self-interstitial atoms in electron-irradiated Al

V. Spirić, L. E. Rehn,\* K.-H. Robrock, and W. Schilling

*Institut für Festkörperforschung der Kernforschungsanlage Jülich, 517 Jülich, Germany*

(Received 10 May 1976)

Application of a highly sensitive elastic-aftereffect technique, capable of resolving changes in strain as small as  $\pm 5 \times 10^{-9}$ , has revealed the existence of an anelastic relaxation process due to the simultaneous migration and reorientation of single interstitials in recovery stage I of low-temperature electron-irradiated Al. Only the  $\langle 100 \rangle$ -split interstitial configuration is consistent with the measured orientational dependence of the relaxation strength in single-crystal samples. The observed anisotropy of the interstitial dipole tensor is small,  $|P_{11} - P_{22}| = 1.1 \pm 0.3$  eV, showing that the long-range displacement field of this defect has nearly cubic symmetry. A comparison of the annealing of the relaxation strength with that of the resistivity shows a transition from correlated to uncorrelated recovery in stage  $I_{D+E}$ . The thermodynamic properties characterizing the single-interstitial relaxation process explain why it has not been observed in previous internal-friction studies.

### I. INTRODUCTION

Irradiation of Al with MeV electrons at low temperatures is known to create vacant lattice sites and self-interstitial atoms (SIA's).<sup>1</sup> Recent experimental evidence overwhelmingly favors the  $\langle 100 \rangle$ -split configuration for the SIA in Al.<sup>2-4</sup> This defect is expected to undergo reorientation only as it migrates through the lattice,<sup>5</sup> and not by means of a simple rotation about its center of mass. Because of the detailed information concerning the symmetry and migration kinetics of a defect which can be obtained through the study of anelastic processes, several attempts have been made to observe an internal-friction peak due to the reorientation of isolated single SIA's in face-centered-cubic metals.<sup>6-8</sup> Although internal-friction peaks due to the interstitial member of close-pair defects have been reported in irradiated Al,<sup>6,7</sup> Cu,<sup>9,10</sup> and Ni,<sup>11</sup> no internal-friction peak associated with the reorientation of isolated single SIA's in face-centered-cubic metals has been correctly identified.

Another method for investigating anelastic processes which, as will be seen below, is more appropriate when defect migration and reorientation occur simultaneously, is the elastic aftereffect (EAE). In this paper, we report EAE measurements on low-temperature electron-irradiated aluminum single crystals. An anelastic relaxation process due to the simultaneous migration and reorientation of single  $\langle 100 \rangle$ -split SIA's has been observed. The kinetics of this process show clearly why it has not been found using internal-friction techniques. Discussion of several other relaxation processes due to clustered SIA's is contained in the following paper.<sup>12</sup>

### II. EXPERIMENTAL

Anelastic relaxation involves the thermally activated stress-induced ordering of defects whose symmetry is lower than that of the host lattice.<sup>13</sup> Under the influence of an applied stress, the energetically equivalent defect orientations in the unstressed crystal can be split. At temperatures high enough to permit motion of the defects between the various orientations, the defects will redistribute themselves among the various orientations, thereby changing the strain distribution in the host lattice. If the relative alignment of the applied stress and defect orientation is altered, the anelastic effects contribute in varying amounts, thus revealing the symmetry axes of the defects.

Two common techniques exist for studying anelastic relaxations. In the EAE method, shown schematically in Fig. 1(a), the sample is held at a fixed temperature and the exponential growth (decay) of the anelastic strain  $\delta\epsilon(t)$ , produced by the relaxing defects, is measured during application (after removal) of a constant stress  $\sigma$ . If  $\epsilon_0$  denotes the instantaneous elastic strain and  $\tau$  is the relaxation time, we have, during loading,

$$\epsilon(t) = \epsilon_0 + \delta\epsilon(t),$$

with

$$\delta\epsilon(t) = \delta\epsilon(\infty)(1 - e^{-t/\tau}).$$

After removal of the stress, which has been applied for a time  $t_0$ , we have

$$\epsilon(t) = \delta\epsilon(t_0)e^{-t/\tau}$$

or

$$\epsilon(t) = \delta\epsilon(\infty)e^{-t/\tau} \text{ for } t_0 \gg \tau.$$

The identical information pertaining to the anelastic process is therefore available in both the loading and unloading curves. However, since the unloading ( $\sigma = 0$ ) curves are free of any elastic-constant changes (e.g., annealing of the diaelastic modulus change)<sup>3</sup> and also of any small deviations in the applied stress, they are both easier to interpret and more accurately measurable than the loading curves. The magnitude of the relaxation strength  $\Delta$  defined as  $\delta\epsilon(\infty)/\epsilon_0$  in single crystals of different orientations furnishes information about the symmetry of the relaxing defects. By making measurements at different temperatures, both the activation energy for reorientation  $H$  and the pre-exponential time constant  $\tau_0$  can be obtained from the relation

$$\tau = \tau_0 e^{H/kT}.$$

Internal friction is certainly the most widely employed method of studying anelastic phenomena. In its most common form, a measurement is made

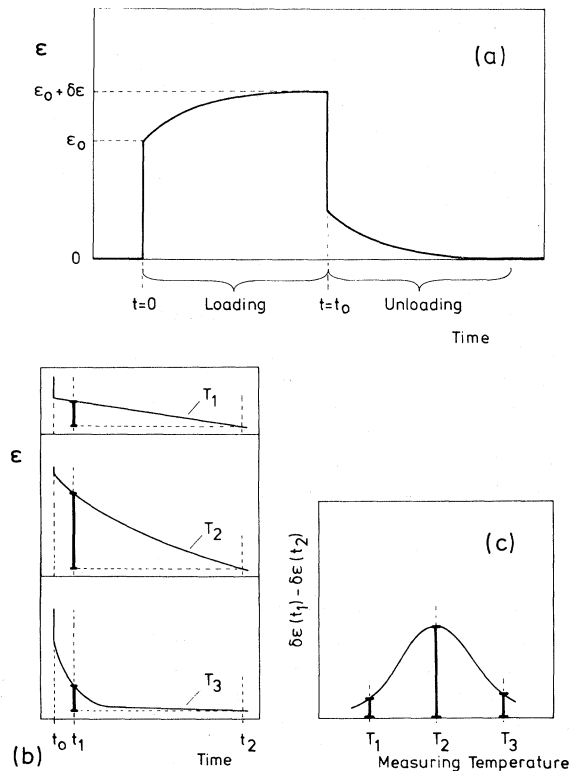


FIG. 1. (a) Schematic diagram of the elastic-aftereffect technique. The existence of an anelastic process is indicated by the appearance of the anelastic strain  $\delta\epsilon$ . (b) Aftereffect curves for three different measuring temperatures  $T_1 < T_2 < T_3$ . The relaxation time is inversely proportional to the measuring temperature. (c) The corresponding isochronal aftereffect curve, showing how the anelastic process manifests itself as a peak.

of the decaying amplitude  $A$  of a freely vibrating specimen. For a single relaxation process, this decay is described by the relation<sup>1,3</sup>

$$A(t) = A_0 e^{-(\Omega/2)Q^{-1}t} \cos \Omega t.$$

$A_0$  is the maximum amplitude of vibration at  $t=0$ , where free decay is assumed to begin. The frequency  $\Omega$  and the damping  $Q^{-1}$  are given by

$$\Omega = \omega \{1 - \frac{1}{2}\Delta [1 + (\omega\tau)^2]^{-1}\},$$

$$Q^{-1} = \Delta \omega \tau / [1 + (\omega\tau)^2].$$

Here,  $\omega$  is the natural frequency of vibration in the absence of any damping. By determining the temperature at which the maximum damping occurs ( $\omega\tau = 1$ ), and noting the temperature shift of the maximum for different frequencies, it is again possible to determine  $\tau_0$ ,  $H$ , and  $\Delta$ . The difference between the two methods is as follows: In an EAE experiment, the small anelastic strain produced by the relaxing defects has to be measured directly. The measuring time is of the order of the relaxation time. With internal friction, the decay of the total strain is the quantity which is directly determined. At the internal-friction peak maximum, the amplitude of this signal is a factor of approximately  $4/\Delta$  larger than the signal in the EAE case. Since  $\Delta$  is almost always  $\ll 1$ , the requirement on sensitivity is much less for an internal-friction experiment, explaining why it is so frequently employed. However, the time constant (i.e., the time for the amplitude to decay to  $1/e$  of its initial value) associated with the internal-friction technique is also larger by the same factor  $4/\Delta$ . For situations where relaxation of the defects may lead simultaneously to their annihilation (i.e., when defect reorientation is accomplished through migration) the longer time constant of the internal-friction technique may prove to be a serious handicap. This can occur, because the larger the number of jumps a defect makes during a measurement, the greater the probability of the defect encountering a reaction partner and disappearing. In other words, the gain in signal strength expected from the internal-friction technique does not materialize, because the larger required number of defect jumps leads to annihilation of the defect species before a measurement can be completed. As will be seen below, this is the reason why the relaxation process from single SIA's has not previously been observed using internal-friction techniques.

In order to achieve the necessary sensitivity in the present investigation, a laser-interferometry technique was employed to measure the strain. Using the Hewlett-Packard system No. 5526, the twist angle of a small mirror mounted on the pendulum could be determined to an accuracy of  $10^{-8}$

rad. This corresponds to a torsional strain in the sample of  $5 \times 10^{-10}$ . Although this high degree of sensitivity could indeed be achieved for short periods of time, it could not be maintained for the full 15–20 min necessary to complete an aftereffect measurement. Due to thermal fluctuations in the cryostat itself and mechanical noise from the environment, the accuracy in determining the twist angle was limited to  $\pm 10^{-7}$  rad, corresponding to an accuracy in  $\epsilon$  of  $\pm 5 \times 10^{-9}$ . Loading strains ( $\epsilon_0$ ) were always  $3 \times 10^{-5}$ .

When the possibility for defect annihilation exists during reorientation, the relaxation strength  $\Delta$  becomes a function of the time. If  $n$  is the average number of reorientation jumps before annihilation, an effective relaxation time  $\tau'$  is measured. Under the assumption that during the measurement  $n$  remains constant,  $\tau'$  is given by

$$\tau' = [n/(n+1)]\tau.$$

Therefore, when the number of defect jumps to annihilation is much greater than one, the measured time constant may be considered to be free of annealing effects. For example, the difference between the real and measured time constants for  $n=20$ , is about 5%.

Measurements were made using an inverted torsion pendulum which has been described in detail elsewhere.<sup>14</sup> The irradiations were performed with 3-MeV electrons generated by the Van de Graaff accelerator at the KFA Jülich.<sup>15</sup>

The samples were hollow tubelike single crystals, 30 mm long and 3 mm in diameter. Specimens with  $\langle 111 \rangle$  and  $\langle 100 \rangle$  torsion axes were spark cut from 99.999% pure Al single-crystal rods. After spark cutting, a surface layer of about 100–150  $\mu\text{m}$  was removed by chemical etching, leaving a final wall thickness of 150–200  $\mu\text{m}$  for the irradiated portion of the sample. The quality of the samples was checked both before and after the experiments by means of Laue x-ray photographs. The torsion axes were all found to be within  $\pm 3^\circ$  of the desired crystallographic directions. The main advantage of this sample form is its mechanical stability. By running liquid helium through the bore of the sample, it was possible to irradiate with a beam current as high as 20  $\mu\text{A}/\text{cm}^2$ , and still maintain the sample temperature below 5 K. The linear decrease of the elastic moduli which was always observed shortly after the onset of irradiation, showed that all dislocation segments had been effectively pinned.<sup>13</sup>

Defect concentrations were monitored by means of two resistivity samples, one located directly in front of the main sample with respect to the electron beam, and one behind. The difference in damage between these two samples was found to be

about 30%. Mohrenstein-Ertel<sup>16</sup> has shown that the decrease in defect concentration along the periphery of the sample to the 30% lower value is linear within  $\pm 5\%$ . Therefore, we estimate the maximum error in using the average of the two resistivity values to determine the defect concentration in the main sample to be  $\pm 2\%$ . There is no influence of the slight inhomogeneity of the damage upon the elasticity measurements, because all portions of the cylindrical sample contribute additively to the total restoring force.

The sample temperature was adjustable over the range from 6 to 300 K, with a stability of  $\pm 0.1$  K/ (30 min). Measurements were performed in the following manner. EAE curves were obtained at selected temperatures up to a certain maximum temperature. The sample was then cooled to 6 K, the remaining residual resistivity was determined and the stepwise procedure was repeated up to a higher temperature. In this way it was possible to study both the growth and decay of the relaxation strength. The relaxation strength  $\Delta$  and the relaxation time  $\tau$  have been determined either directly from the EAE curves, or from their derivatives. The latter procedure is usually preferred, since it eliminates any drift of the zero point of the EAE curve which may have occurred during the measurement.

A useful means of presenting the many time-dependent aftereffect curves obtained in the present experiment is in the form of so-called isochronal aftereffect curves, shown schematically in Figs. 1(b) and 1(c). The total amount of anelastic strain measured between two freely chosen but fixed times  $t_1$  and  $t_2$  is plotted as a function of the measuring temperature  $T$ . The occurrence of a peak reveals the existence of a relaxation process in the indicated temperature regime. For  $t_1=30$  sec and  $t_2=300$  sec, as used in the present experiments, the peak maximum occurs for  $\tau \cong 100$  sec.

### III. RESULTS AND DISCUSSION

Two single-crystal aluminum samples, one possessing a  $\langle 111 \rangle$  and the other a  $\langle 100 \rangle$  torsion axis, were irradiated to resistivity changes of 270 and 170  $\text{n}\Omega/\text{cm}$ , respectively. Isochronal aftereffect curves for the  $\langle 111 \rangle$  sample obtained at various stages in the annealing program are shown in Fig. 2. Of particular interest to the present discussion is peak A, which appears in Fig. 2 at 37.5 K. Characteristics of the two neighboring processes 2 and 4 are discussed in detail in the following paper.<sup>12</sup>

The behavior of peak A after different annealing temperatures indicates that the defect responsible for this anelastic process anneals in the same temperature regime where the peak occurs. In order

to show the annealing behavior of process A in greater detail, the relaxation strength observed at a reference temperature of 37 K is plotted in Fig. 3(a) as a function of the residual resistivity measured at 6 K after each annealing temperature. Process A anneals completely in stage  $I_{D+E}$  ( $0.7 \geq \Delta\rho/\Delta\rho_0 \geq 0.5$ ). This stage is due to the recombination of freely migrating single interstitials with immobile vacancies. Its separation into correlated ( $I_D$ ) and uncorrelated ( $I_E$ ) recovery occurs only for much lower defect concentrations.<sup>1</sup> The annealing of process A parallels the resistivity recovery in stage  $I_{D+E}$ , indicating that its relaxation strength is proportional to the concentration of single SIA's present in the sample. Therefore, process A is attributed to the anelastic relaxation of single SIA's.

It is apparent from Fig. 3(a) that a small portion of the relaxation strength measured at 37 K is due to defects which do not anneal until the middle of stage II. The time constant (50 sec) for this background at 37 K is quite different from that of pro-

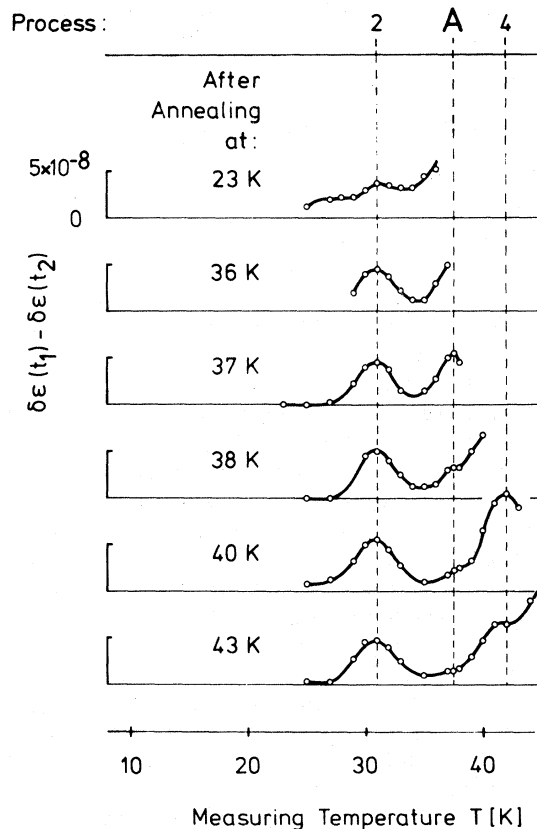


FIG. 2. Isochronal elastic-aftereffect curves for a  $\langle 111 \rangle$  oriented crystal irradiated to a Frenkel pair concentration of approximately  $7 \times 10^{-4}$ . Each curve is labeled by the maximum annealing temperature attained prior to its measurement.

cess A (160 sec). Part of this background effect is due to the two neighboring processes, but other effects are apparently also contributing which cannot be individually separated because of the small magnitude of the total background effect.

In order to investigate the symmetry of the interstitial defects responsible for peak A, similar measurements were made on a  $\langle 100 \rangle$  oriented crystal. The annealing of the relaxation strength measured at the reference temperature of 37 K for this sample is shown in Fig. 3(b). No indication for a process which anneals systematically in stage  $I_{D+E}$  is found in the  $\langle 100 \rangle$  sample. However, a background effect similar to that found in the  $\langle 111 \rangle$  orientation is again present.

The difference between process A and the background effect shown in Fig. 5(b) also manifests itself if aftereffect curves are measured at different temperatures. Figure 4 shows the results obtained at 36, 37, and 37.5 K. As expected for a simple relaxation process, a strong temperature dependence is found for the relaxation time in the  $\langle 111 \rangle$  sample. On the other hand, for the  $\langle 100 \rangle$  sample which does not exhibit process A but only the background process, no significant temperature dependence of the time constant is observed. Figure 5 shows the difference between process A and the background effect from yet another perspective. Here, the aftereffect curves for both crystal orientations, observed at 37 K after annealing at 36, 38, and 40 K, are given. Again, no systematic annealing of the total relaxation strength occurs for the  $\langle 100 \rangle$  sample, although it is clearly evident in the  $\langle 111 \rangle$  orientation. Process A, which occurs at 37 K with a time constant of 160 sec, disappears completely after annealing at 40 K. A smaller effect then remains, which like the effect in the  $\langle 100 \rangle$  crystal possesses a much faster time constant (50 sec) and which anneals at a much higher temperature. In other words, there is no detectable relaxation process from single intersti-

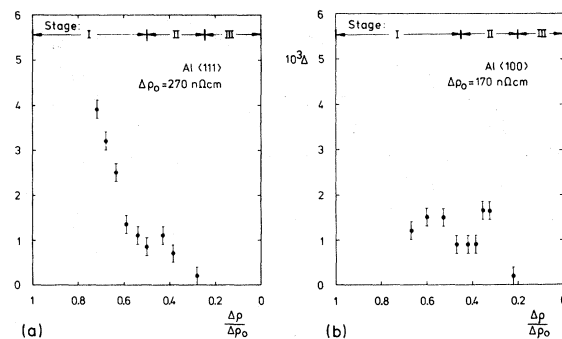


FIG. 3. Total relaxation strength  $\Delta = \Delta\epsilon/\epsilon_0$  observed at 37 K, vs the remaining fractional resistivity change  $\Delta\rho/\Delta\rho_0$  for (a) the  $\langle 111 \rangle$  and (b) the  $\langle 100 \rangle$  sample.

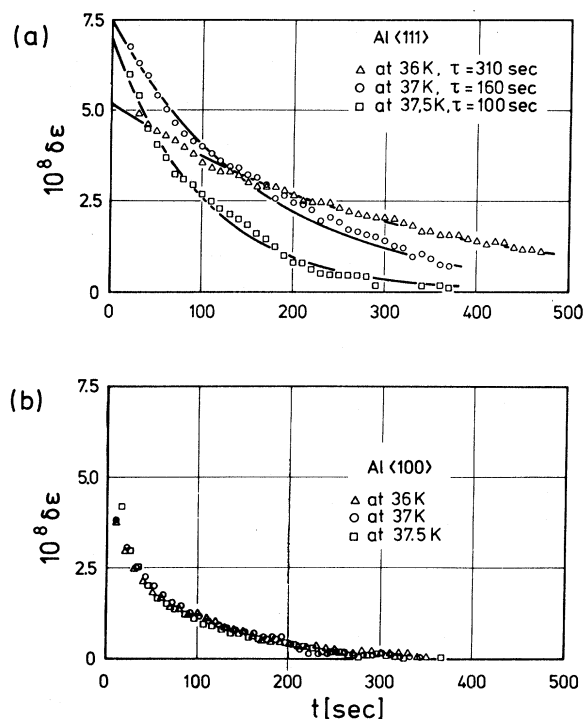


FIG. 4. Elastic-aftereffect curves measured at 36, 37, and 37.5 K after annealing at 37 K for (a) the  $\langle 111 \rangle$  and (b) the  $\langle 100 \rangle$  sample.

tials in the  $\langle 100 \rangle$  oriented crystal. From the absence of the relaxation effects due to single interstitials in the  $\langle 100 \rangle$  crystal in Al, it follows directly that the SIA must have either tetragonal or  $\langle 100 \rangle$  orthorhombic symmetry. Of the several proposed configurations for the SIA in fcc metals,<sup>4</sup> only the  $\langle 100 \rangle$ -split configuration is consistent with this symmetry restriction.<sup>13</sup> This result is in agreement with diffuse x-ray<sup>2,4</sup> and diaelastic modulus measurements,<sup>3</sup> in which the  $\langle 100 \rangle$ -split configuration has also been shown to be the stage I interstitial in Al.

A convenient means of characterizing the elastic behavior of a defect in a host crystal has been outlined by Kröner,<sup>17</sup> who first introduced the term "elastic dipole." In this formalism, the defect is described by a tensor  $P_{ij}$  whose elements are defined as the stresses  $\sigma_{ij}$  needed to maintain constant strain per unit concentration  $N$  of defects. Thus,

$$P_{ij} \equiv \frac{\partial \sigma_{ij}}{\partial N}.$$

If the concentration of defects is known, then the anisotropy  $|P_{11} - P_{22}|$  of the dipole force tensor

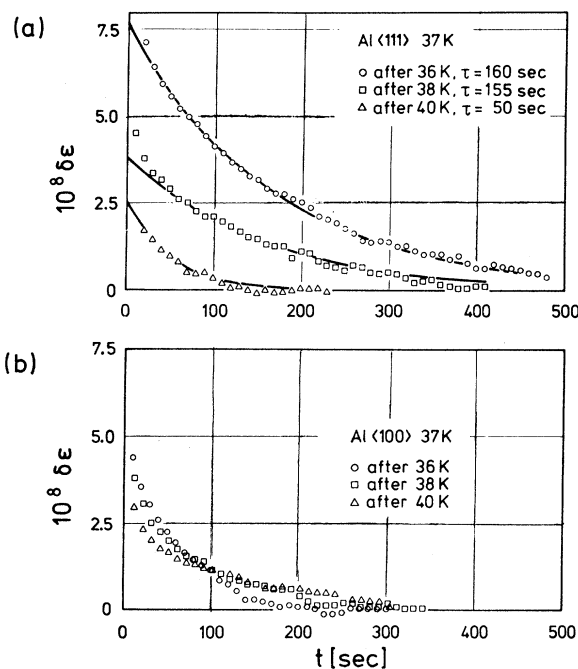


FIG. 5. Elastic-aftereffect curves measured at 37 K, after annealing at 36, 38, and 40 K for (a) the  $\langle 111 \rangle$  and (b) the  $\langle 100 \rangle$  samples.

characterizing the tetragonal interstitial

$$\begin{pmatrix} P_{11} & 0 & 0 \\ 0 & P_{22} & 0 \\ 0 & 0 & P_{22} \end{pmatrix}$$

can be calculated<sup>13</sup> from the relaxation strength of process A.

However, caution must be exercised in using the measured resistivity changes to determine the concentration of single SIA's. Only single interstitials contribute to the mechanical relaxation process A, but the resistivity is not so selective. The amount of resistivity remaining in the sample is a measure of the total defect concentration and contains a contribution from any clusters which may have already formed during the annealing. It therefore gives only an upper limit on the total single interstitial concentration remaining in the sample. On the other hand, the observed reduction of the residual resistivity in stage I does not include the single interstitials which disappear by clustering. It therefore gives only a lower limit on the single interstitial concentration which has disappeared. Thus by using the amounts of relaxation strength and resistivity which remain, a lower limit for  $|P_{11} - P_{22}|$  can be calculated, while the combination of annealed relaxation strength and annealed resistivity produces an upper bound. In this man-

ner, using a resistivity change of  $4\text{-}\mu\Omega\text{ cm/at.}\%$  defects,<sup>2</sup> a value of

$$|P_{11} - P_{22}| = 1.1 \pm 0.3 \text{ eV}$$

is found. Despite the large error bars arising from the uncertainty in the single SIA concentration, the value given here is considerably more precise than that determined by diffuse x-ray measurements. It is in good agreement with both theoretically calculated values<sup>18</sup> and the less precise values determined from x-ray measurements.<sup>2</sup>

The magnitude of  $|P_{11} - P_{22}|$  for the  $\langle 100 \rangle$ -split interstitial is relatively small, as compared for example with a value of 6.0 eV for carbon in iron,<sup>19</sup> indicating that the long-ranging displacement field around the single interstitial has nearly cubic symmetry. If central forces are used to describe the interactions between the two  $\langle 100 \rangle$ -split dumbbell atoms and their nearest neighbors, the long-ranging displacement field becomes exactly cubic when the distance  $d$  between the two dumbbell atoms is equal to one-half of a lattice constant  $a$ . A value for  $|P_{11} - P_{22}|$  of 1.1 eV is consistent with a value for  $d$  of either  $0.4a$  or  $0.6a$ .

An activation analysis for process A is shown in Fig. 6, where the measured relaxation time  $\tau$  is plotted as a function of the reciprocal measuring temperature  $1/T$ . The slope and  $\tau_0$  intercept for the resulting straight line giving values of

$$H = 0.115 \pm 0.025 \text{ eV} \quad \text{and} \quad \tau_0 = 3 \times 10^{-14} \pm 3 \text{ sec}$$

for the activation energy of reorientation and pre-exponential time constant, respectively. This activation energy is the same as that reported<sup>20</sup> for resistivity annealing in stage  $I_{D+E}$ , indicating that both reorientation and migration of the interstitial

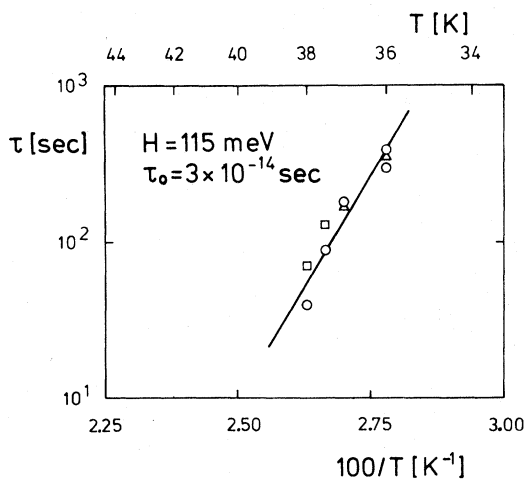


FIG. 6. Arrhenius diagram of the relaxation time for process A.  $\Delta$ , measured after annealing at 36 K;  $\circ$ , after 37 K;  $\square$ , after 38 K.

occur by the same jump process. Indeed, model calculations<sup>5</sup> have shown that the jump process illustrated in Fig. 7, in which the  $\langle 100 \rangle$ -interstitial center of mass migrates to a next-nearest-neighbor position while its axis undergoes a rotation of  $90^\circ$ , has the lowest activation energy. Reorientation without migration requires a considerably higher activation energy. The failure to observe a single interstitial relaxation process at a temperature below that of free interstitial migration in the present study, or by authors using internal-friction techniques,<sup>6-8,12</sup> also supports this conclusion.

If  $n$  is the average number of jumps a single interstitial makes before reacting with another defect and disappearing, then the time constant  $\tau_a$  for annealing of the relaxation strength is  $\tau_a = n\tau$ , where  $\tau$  is the time constant for one jump. From the present annealing results for  $\Delta$ , a value of  $n \approx 10$  is found in about the middle of stage  $I_{D+E}$ , which increases to  $n \approx 100$  near the end. A similar analysis of stage  $I_D$  using the resistivity recovery also gives  $n \approx 10$  in the middle of stage  $I_{D+E}$ , but this increases to  $n \approx 500$  near the end. The reason for this behavior is quite simple. All jumps leading to reactions of single interstitials with other defects contribute to the annealing of  $\Delta$ . However, the resistivity annealing counts only those jumps which lead to the recombination of interstitials with vacancies. The equality of the values in the middle of stage  $I_{D+E}$  can thus be attributed to the predominance of correlated recovery (recombination of SIA's with their own vacancies). In the uncorrelated recovery which occurs toward the end

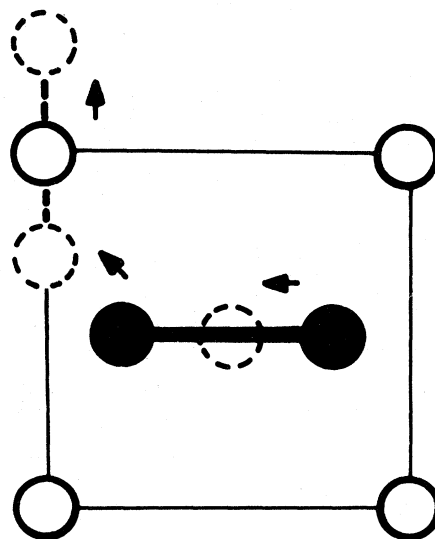


FIG. 7. Jump process for a  $\langle 100 \rangle$ -split interstitial in the fcc lattice. Migration and reorientation occur simultaneously.

of the stage, the greater number of effective reaction partners (vacancies *and* interstitials) seen with the relaxation strength produces a smaller value of  $n$ . Of course the error limits associated with this calculation are large, but the values given here should be approximately correct.

The small number of jumps which a single interstitial makes before disappearing accounts for the fact that the interstitial reorientation during migration has not previously been observed with internal-friction techniques. Using a defect concentration for which the relaxation strength of process  $A$  is  $4 \times 10^{-3}$  (as in the present study), we see from Sec. II that the associated internal-friction decay would occur with a time constant of about  $10^3 \tau$ , where  $\tau$  is again the time constant for defect reorientation. If the single SIA's would not disappear during migration, the amplitude of free vibration would decay to  $1/e$  of its original amplitude after each defect had made an average of  $10^3$  jumps. Full advantage could then be taken of the larger internal-friction signal. However, we have seen above that practically all of the single SIA's have already disappeared after an average of only 100 jumps. The associated internal-friction effect could therefore be detected only if the sensitivity of the internal-friction apparatus was made comparable to that of the present EAE technique. In that case, it would be possible to determine  $Q^{-1}$  after only a few (3–5) defect jumps, i.e., before many of the defects had disappeared. Such a high degree of sensitivity in the measurement of strain is, however, not presently available using internal-friction techniques.

#### IV. CONCLUSIONS

Application of a highly sensitive elastic-after-effect technique (capable of detecting changes in strain as small as  $5 \times 10^{-9}$ ) to the study of low-temperature electron-irradiated aluminum has revealed the existence of a previously unobserved anelastic relaxation process, called process  $A$ .

(i) Process  $A$  was found to occur only during single interstitial migration in stage  $I_{D+E}$ . In addition, its annealing is seen to parallel the resistivity recovery in stage  $I_{D+E}$ , demonstrating that the relaxation strength of this process is proportional to the concentration of single self-interstitials present

in the sample. For these reasons, process  $A$  has been attributed to the anelastic relaxation of single self-interstitial atoms.

(ii) Of all the proposed stable self-interstitial configurations in a face-centered-cubic lattice,<sup>4</sup> only the tetragonal  $\langle 100 \rangle$ -split configuration is in agreement with the present measurements of the orientation dependence of the relaxation strength of stage-I interstitials.

(iii) The measured activation energy and pre-exponential time constant for process  $A$  are the same, within experimental error, as those reported<sup>20</sup> for resistivity annealing in stage  $I_{D+E}$ , indicating that single interstitial reorientation and migration occur by the same jump process.

(iv) The anisotropy of the dipole tensor characterizing the long-ranging strain field of the  $\langle 100 \rangle$  single interstitial is small ( $\sim 1$  eV). This implies a separation between the two atoms which form the interstitial of either 0.4 or 0.6 times the lattice constant.

(v) The observed ratio of the number of jumps executed by a single interstitial before encountering a vacancy (resistivity annealing) to the number executed before encountering any reaction partner (relaxation strength annealing) is in agreement with the interpretation of recovery stage  $I_{D+E}$  in terms of a transition from correlated to uncorrelated annealing.

(vi) The thermodynamic properties of process  $A$  show why it has not been observed using internal-friction methods. Since long-range migration and reorientation<sup>1</sup> occur simultaneously, the single interstitial configuration disappears through reactions with other defects in the lattice in a time which is short compared to that necessary for an internal-friction measurement. The success of the elastic after effect method is due to the fact that this experimental technique requires only a few (3–5) defect jumps for a complete determination of the properties of an anelastic process.

#### ACKNOWLEDGMENTS

The authors would like to thank Dr. P. H. Dederichs and Dr. H. R. Schober for many helpful discussions. The technical assistance of Frau I. Serpekian is also gratefully acknowledged. We thank F. W. Young, Jr. for a careful reading and discussion of the manuscript.

\*Present address: Materials Science Division, Argonne National Laboratory, Argonne, Ill. 60439.

<sup>1</sup>*Vacancies and Interstitials in Metals*, edited by A. Seeger, D. Schumacher, W. Schilling, and J. Diehl (North-Holland, Amsterdam, 1970).

<sup>2</sup>P. Ehrhart and W. Schilling, *Phys. Rev. B* **8**, 2604

(1973).

<sup>3</sup>K.-H. Robrock and W. Schilling, *J. Phys. F* **6**, 303 (1976).

<sup>4</sup>P. Ehrhart, H.-G. Haubold, and W. Schilling, *Adv. Solid State Phys.* **XIV**, 87 (1974).

<sup>5</sup>J. B. Gibson, A. N. Goland, M. Milgram, and G. H.

- Vineyard, Phys. Rev. 120, 1229 (1960); P. H. Dederichs, C. Lehmann, and A. Scholz, Phys. Rev. Lett. 31, 1130 (1973).
- <sup>6</sup>K. Ehrensberger, V. Fischer, J. Kerscher, and H. Wenzl, J. Phys. Chem. Solids 31, 1835 (1970).
- <sup>7</sup>M. Riggauer, W. Schilling, J. Völkl, and H. Wenzl, Phys. Status Solidi 33, 843 (1969).
- <sup>8</sup>D. König, J. Völkl, and W. Schilling, Phys. Status Solidi 7, 591 (1964).
- <sup>9</sup>R. L. Nielsen and J. R. Townsend, Phys. Rev. Lett. 21, 1749 (1968).
- <sup>10</sup>J. Holder, A. V. Granato, and L. E. Rehn, Phys. Rev. B 10, 363 (1974).
- <sup>11</sup>G. de Keating-Hart, R. Cope, C. Minier, and P. Moser, Jülich Conf. 1, 327 (1968).
- <sup>12</sup>K.-H. Robrock, L. E. Rehn, V. Spirič, and W. Schilling, following paper, Phys. Rev. B 15, 680 (1977).
- <sup>13</sup>A. S. Nowick and B. S. Berry, *Anelastic Relaxation in Crystalline Solids* (Academic, New York, 1972).
- <sup>14</sup>K.-H. Robrock, Report of the Kernforschungsanlage, Jülich, Germany, Report No. Jül-1088-FF, 1974 (unpublished).
- <sup>15</sup>J. Hemmerich, Report of the Kernforschungsanlage, Jülich, Germany, Report No. Jül-579-FN, 1969 (unpublished).
- <sup>16</sup>M. Mohrenstein-Ertel, Diplomarbeit (Aachen: RWTH Aachen, 1969) (unpublished).
- <sup>17</sup>E. Kröner, *Kontinuumstheorie der Versetzungen und Eigenspannungen* (Springer, Berlin, 1958).
- <sup>18</sup>A. Seeger, E. Mann, and R. V. Jan, J. Phys. Chem. Solids 23, 639 (1962).
- <sup>19</sup>H. Ino and Y. Inokuti, Acta Met. 20, 157 (1972).
- <sup>20</sup>H. M. Simpson and A. Sosin, Radiat. Eff. 3, 1 (1970).